Preparation process, crystal structure, and physical properties of the 110-K single-phase Pb-Bi-Sr-Ca-Cu-O superconductor

F. Shi
Department of Materials Science and Engineering, University of Science and Technology, Beijing, Beijing, 100083, China

T. S. . Rong
Department of Metal Physics, University of Science and Technology, Beijing, Beijing, 100083, China

S. Z. Zhou
Department of Materials Science and Engineering, University of Science and Technology, Beijing, Beijing, 100083, China

X. F. Wu
Department of Metal Physics, University of Science and Technology, Beijing, Beijing, 100083, China

J. Du and Z. H. Shi
Department of Materials Science and Engineering, University of Science and Technology, Beijing, Beijing, 100083, China

C. G. Cui, R. Y. Jin, J. L. Zhang, and Q. Z. Ran
Institute of Physics, Academia Sinica, Beijing, China

N. C. Shi
China University of Geoscience, Beijing, 100083, China
(Received 2 October 1989)

The high-T_c (110-K) superconducting phase in the Pb-Bi-Sr-Ca-Cu-O has been isolated and its structural and physical properties investigated. Transmission-electron-microscopy results show that the structure belongs to a monoclinic system that is different from reports by other groups and in agreement with our x-ray-diffraction analysis. The refined crystal data are $a=3.779$ Å, $b=3.834$ Å, $c=37.150$ Å, $\alpha=\beta=90°$, $\gamma=90°\ 51'$, $V=538.5$ Å^3, space group $I112$. Based on the resistivity, magnetization, critical-field, and specific-heat measurements, various parameters characterizing the monophase superconductors were determined or derived. Some of them are listed as follows: T_{ce} (endpoint) = 107 K, T_{cm} (midpoint) = 110 K, ΔC (specific heat jump at 107 K) = 5.3 J/mol K, γ (the Sommerfeld constant) = 34.6 mJ/mol K^2, Θ (Debye temperature) = 418 K, $H_{c1}(0)=900$ G, $H_{c2}(0)=184$ T, and $J_c(1.5\text{ K}, 0\text{ T})=4.8\times10^4$ A/cm^2, etc. Morphology, thermal analysis, and pressure effects of the sample are also mentioned.

I. INTRODUCTION

Since the initial work performed by Bednorz and Muller[1] in 1986, a variety of copper oxides with high superconducting transition temperature, such as those of the Bi-Sr-Ca-Cu-O (Ref. 2) and Tl-Ba-Ca-Cu-O,[3] have been discovered. In the Bi-Sr-Ca-Cu-O, three superconducting phases[2,4-6] have been identified as $Bi_2Sr_2CuO_6$ (2:2:0:1 phase, $T_c\sim10$ K), $Bi_2Sr_2CaCu_2O_8$ (2:2:1:2 phase, $T_c\sim85$ K), and $Bi_2Sr_2Ca_2Cu_3O_{10}$ (2:2:2:3 phase, $T_c\sim110$ K). The three phases are usually believed to have basically tetragonal or orthorhombic crystallagraphic structures with lattice parameters c of 24, 30, and 37 Å, and to have single, double, and triple layers of CuO_2 planes located between two Bi_2O_2 layers, respectively. It is well known that the 10-K and the 85-K phases are easily obtained by the ordinary process, but it is difficult to synthesize the 110-K single phase because its growth condition is critical. That is why there is little information on the 2:2:2:3 phase up to now.

During the period from July to September in 1988, having found the partial substitution of Pb for Bi in the system beneficial to cut the "resistance tail" and/or raise the volume fraction of the 110-K phase, we[7] succeeded independently in isolating the 110-K phase with ordinary process, by adding more Ca and Cu based on $Bi_2Sr_2Ca_2Cu_3O_{10}$ and improving the heat treatment conditions (almost simultaneously Kawai *et al.*[8] also demonstrated that the solid reaction under low-oxygen pressure of $\frac{1}{13}$ atom, using the codecomposition of metal nitrates, led to the single 110-K phase). Subsequently, we studied the monophase sample structurally, electrically, magnetically, and calorimetrically. Some of the preliminary analyses have been described in previous letters.[7,9] The systematic and latest results are mainly reported in this comprehensive paper.

II. SYNTHESIS, RESISTANCE, AND MORPHOLOGY

The samples were prepared from powders of PbO, Bi_2O_3, $SrCO_3$, $CaCO_3$, and CuO mixed in atomic ratio of

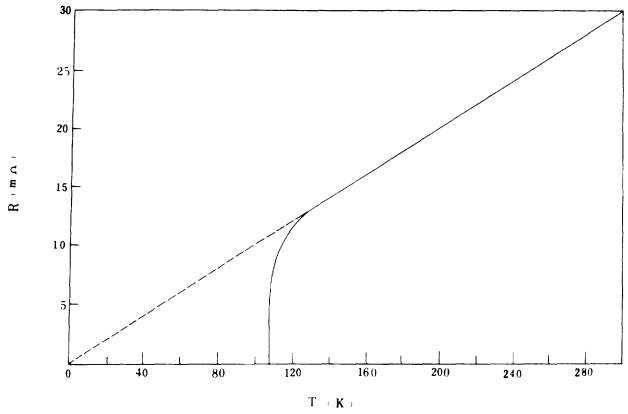

FIG. 1. Temperature dependence of resistance of the sample.

Pb:Bi:Sr:Ca:Cu=3:17:20:30:40. The mixture was calcined at 800–810 °C for 12 h, then reground and pressed into pellets of 16 mm in diameter and 2 mm in thickness at a pressure of 2.5×10^{8} Pa. The pellets were fired at 870–880 °C for (60+180) h in air, followed by furnace cooling to 500 °C and then air quenched to room temperature.

Resistance transitions were measured by the four-probe method at fixed fields in a cryostat in which temperature can be controlled by using a capacitance controller. High quality Ag paste was used for terminal contacts. The current perpendicular to the applied field was 2 mA, corresponding to a current density of 50 mA/cm^2. The temperature was measured by using a calibrated carbon-glass thermometer.

The resistance versus temperature for the sample under zero magnetic field is presented in Fig. 1. It shows that superconducting transition temperature T_{cm} (midpoint of the transition) is 110 K. The resistance became zero at 107 K in the region of sensitivity of 2×10^{-8} V. A quite good relation of linearity between the resistance and temperature at normal state can be found (when extrapolating the curve between the resistance and temperature, it nearly extends to the origin).

Microstructure observation was done by using Cambridge-S250 scanning electron microscopy (SEM). The SEM photos of two fractured surfaces (a),(b) with different magnifications and a free surface (c) for the sample are shown in Fig. 2. Obviously, the matrices are composed of thin plate-like grains with about several tens of microns. It is worth noticing that the inner morphology [Fig. 2(b)] looks more homogeneous and cleaner than the outer one [Fig. 2(c)]; however, the latter looks more compact and/or has better connectivity of grains than the former. It may be due to the volatility differences of Pb and/or other elements between the inner and outer of the samples, which is an important factor to be controlled in the process of fabricating the higher quality samples.

III. MAGNETIC MEASUREMENTS

The magnetization measurements were made on a magnetometer in which the magnetic field can be varied

FIG. 2. SEM photos of the sample: (a) fractured surface with higher magnification; (b) fractured surface with lower magnification; (c) free surface with the same magnification as photo (b).

from 0 to 8 T continuously. A cylindrical sample with $\phi2.0\times5$ mm was used. The temperature was determined by calibrated Pt and carbon thermometer. The experimental error of the magnetization was less than 5×10^{-4} emu.

Figure 3 shows the relation of low field (H to be 100 G) magnetization and temperature of the sample. After the sample had been zero field cooled, the diamagnetic shielding was measured at a fixed field of 100 G with increasing temperature. The Meissner flux expulsion was measured at same field with decreasing temperature and expressed about 25% of this diamagnetic shielding. No step corresponding to the low-T_c phases was observed on

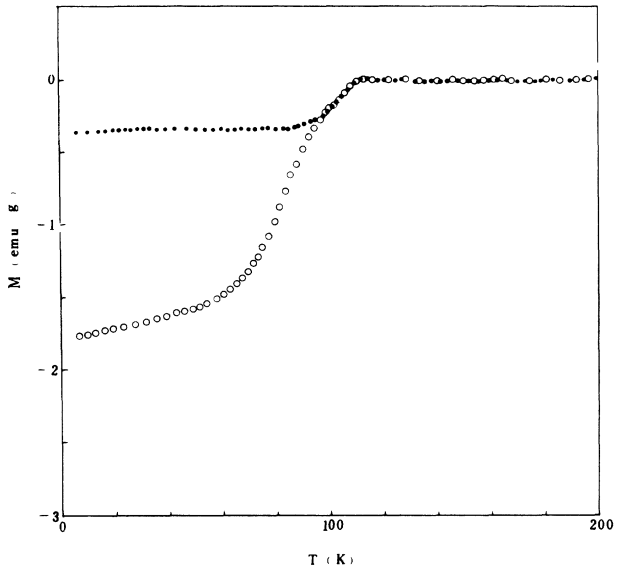

FIG. 3. Magnetization vs temperature for the sample. Both dc screening (open circles) and Meissner effect (solid circles) curves are shown.

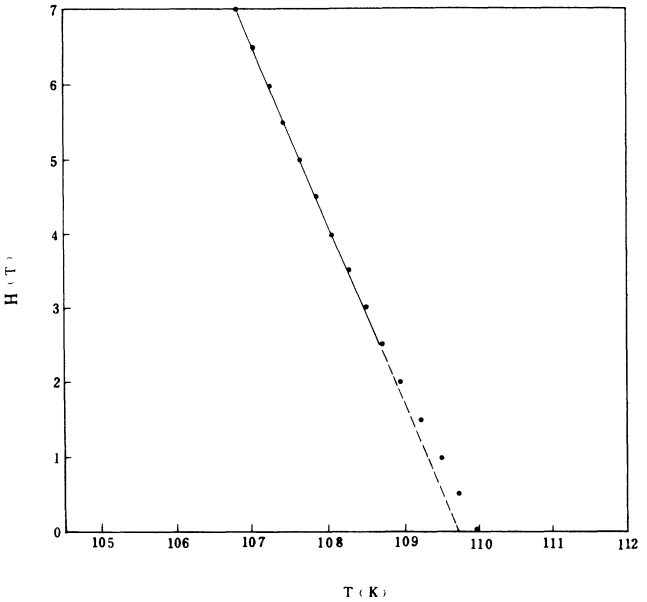

FIG. 5. Magnetic field dependence of superconducting transition temperature near T_{cm}.

the curve. It shows that there is only one high-T_c phase in the sample. The results of the low field magnetization also show that the temperature of superconducting onset is 107 K.

The magnetic hysteresis loop from 50 G to 60 kG for the sample at 1.5 K is shown in Fig. 4. This is a highly symmetric curve. Critical current density $J_c(T=1.5$ K, 0 T) is estimated to be 4.8×10^4 A/cm^2 by the formula $J_c=30$ M/R. The value of dc susceptibility x at 1.5 K can be derived from the loop and easily plotted[10] as a function of magnetic field. It is found that the value of x increases with increasing applied field from 50 to 460 G, then it increases very slowly at field lower than 600 G. After that, it shows a sharp increase. The field 600 G can be regarded as the lower critical field. Because the shape of superconducting grains of the sample can be considered as a sphere, the demagnetization factor can be taken as approximately $\frac{3}{2}$. Then H_{c1} (1.5 K)=900 G.

Figure 5 shows dependence of T_{cm} versus H where T_{cm} is the temperature at which the resistance dropped to 50% of the residual resistance. Critical field slope, $(dH_{c2}/dT)_{T_c}=-2.43$ T/K, was determined by computer using the least-squares fitting of straight line to the experimental data points (3–7 T). Using the Werthamer, Helfand, Hohenberg (WHH) expression in the dirty limit $H_{c2}(0)=-0.693T_c(dH_{c2}/dT)_{T_c}$, the $H_{c2}(0)=184$ T is determined. Furthermore, according to relations of $H_{c2}(0)=\phi_0/(2\pi\xi_0)$, $H_{c1}=[\phi_0/(2\pi\lambda_0^2)]\ln(\lambda_0/\xi_0)$, $K_0=\lambda_0/\xi_0$, and $H_c(0)=H_{c2}/(\sqrt{2}K_0)$, it can be derived in turn that ξ_0 (coherence length)=13.5 Å, λ_0 (penetration depth)=880 Å, $K_0=65$, and $H_c(0)=2$ T.

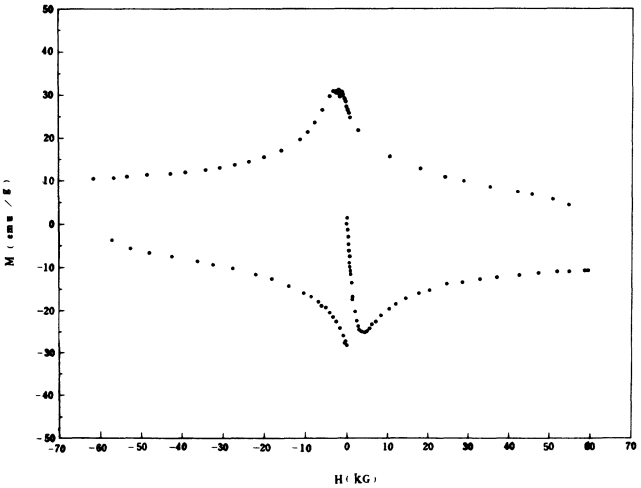

FIG. 4. Magnetization hysteresis loop at 1.5 K.

IV. SPECIFIC HEAT

The specific heat was measured with a scanning method. Figure 6 shows the temperature dependence of the specific heat between 90 and 135 K. It is observed that the specific-heat curve deviates from its original path below 122 K, just as the resistance begins to decrease rapidly around 125 K in the R-T curve. This elucidates that superconducting electrons appear at this temperature, but it must be only a small part of the total. When the temperature decreases to 107 K, the specific heat shows a pronounced jump ΔC, at the temperature corresponding to the onset transition of the magnetic susceptibility, and the zero-resistance temperature. This implies that most of the material becomes superconducting at this temperature.

The existence of the specific heat jump ΔC suggests

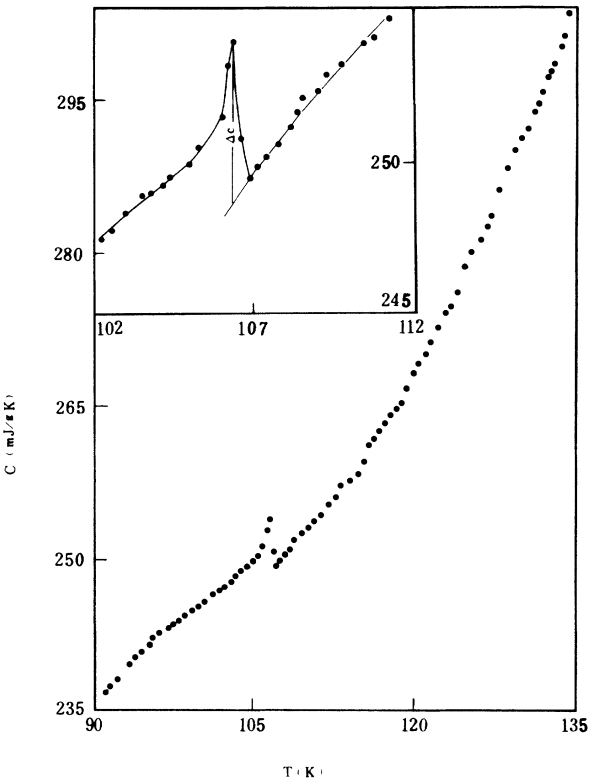

FIG. 6. The specific heat between 90 and 135 K. The inset shows the detailed behavior in the vicinity of T_c.

that the Pb-Bi-Sr-Ca-Cu-O superconductor exhibits bulk superconductivity similar to the Y-Ba-Cu-O superconductor. Some samples[11–13] did not exhibit the jump at T_c; the possible reasons may be that (1) the transition is very broad; (2) the superconducting volume fraction is small and the lattice specific heat is very large around T_c; (3) several phases coexist in a sample and the differences of transition temperatures T_c are small. The value of jump ΔC at T_c can indicate the superconducting fraction relatively. Supposing the molecular weight of $(Pb,Bi)_2Sr_2Ca_2Cu_3O_{10+\delta}$ is 1023 g, the apparent specific heat jump value $\Delta C=5.2$ mJ/g K or 5.3 J/mol K was obtained at T_c in Fig. 6; it is close to the anomaly of the Y-Ba-Cu-O sample, but here the jump is sharper.

At the transition temperature $T_c=107$ K, the specific heat is $C(T_c)=255$ J/mol K, so we can obtain the value $\Delta C/C=2.15$ and $\Delta C/T_c=49.5$ mJ/mol K^2. In the weak coupling BCS limit, the Sommerfeld constant is evaluated to be $\gamma=34.6$ mJ/mol K^2. It seems close to the value of the $Y_1Ba_2Cu_3O_{7-\delta}$ superconductor.[14,15]

The lattice specific heat can be described by the Debye function. The Debye temperature can be estimated by fitting the experimental data with the theoretical Debye function. Neglecting the electron's contribution, the Debye temperatures calculated at different temperatures (from T_c to 133 K) are close to a constant. Its average value is $\Theta=418$ K, approaching the results of $La_{1.85}Sr_{0.15}CuO_4$ and $Y_1Ba_2Cu_3O_{7-\delta}$ superconductors.

V. CRYSTAL STRUCTURE ANALYSIS

The study on structural features of the 110-K phase were done by means of transmission-electron microscopy (TEM) and powder x-ray diffraction (XRD).

The specimen analyzed with TEM was prepared by ion milling or the usual method, i.e., the superconducting sample was crushed and then mounted onto a holey carbon film. The TEM experiments were carried out in a JEOL 2000-FX. By tilting the specimen, a set of selected area diffraction (SAD) patterns were obtained (Fig. 7). As being constructed of the SAD patterns, the reciprocal lattice can be understood.[9] Within the accuracy of SAD, it was determined, when the commensurate and incommensurate modulated structures were neglected, that the crystal belongs to the one-face centered monoclinic structure (this conclusion was also supported by convergent beam electron diffraction results[9]). But for easy comparison with other types of perovskite structure superconductors, an I-center sublattice unit cell with $a=3.78$ Å, $b=3.83$ Å, $c=37.1$ Å, and $\gamma=91.2°$ was selected. The more accurate results are given by the following XRD analysis.

Powder x-ray diffractions were taken on a Rigaku rotating anode x-ray diffractometer of D_{max}/RC with CuK_α, 50 kV, 110 mA, scanning speed 1°/min, scanning range 3°–70° (2θ). The XRD pattern of the sample is shown in Fig. 8. Assignment of the XRD and the least-squares refinement of unit cell were carried out by the APPLEMAN program (No. 9214). The unit cell parameters obtained finally are as follows: $a=3.779$ Å, $b=3.834$ Å, $c=37.150$ Å, $\alpha=\beta=90°$, $\gamma=90°$ 51′, $V=538.1$ Å^3, and the space group $I112$. The coincidence between observed d values and calculated d values is satisfactory. The frequent ($00l$) reflections in the XRD pattern indicate that the crystal possesses strong layer structure character. Further studies on the modulation structure are in progress.

VI. FINAL REMARKS

The formation process of the 110-K phase has been investigated systematically. It is found that the sample of good purity can also be obtained from another starting composition $Pb_{0.4}Bi_{1.6}Sr_2Ca_3Cu_4O_y$ as well as $Pb_{0.3}Bi_{1.7}Sr_2Ca_3Cu_4O_y$; the effect of cooling rate after sintering on the sample is complicated. In the study of differential scanning calorimetry (DSC), two endothermal peaks appearing around 288 °C and 495 °C were discovered on the increasing temperature curve of the single-phase sample; however, on the decreasing temperature DSC curve, one unusual heat absorption process occurred from 570 °C to 314 °C and the peak minimum was located at about 514 °C. According to results made by Chen *et al.*,[16] the above phenomena may correspond to the adjustment of the modulated structure. Differential thermal analysis (DTA) shows that the melting point (defined as the onset temperature of the endothermal peak) of the 110-K phase is 875 °C, but the peak minimum temperature is as high as 886 °C. All of these results suggest that the preparation process of the single 110-K phase given in this paper is reasonable.

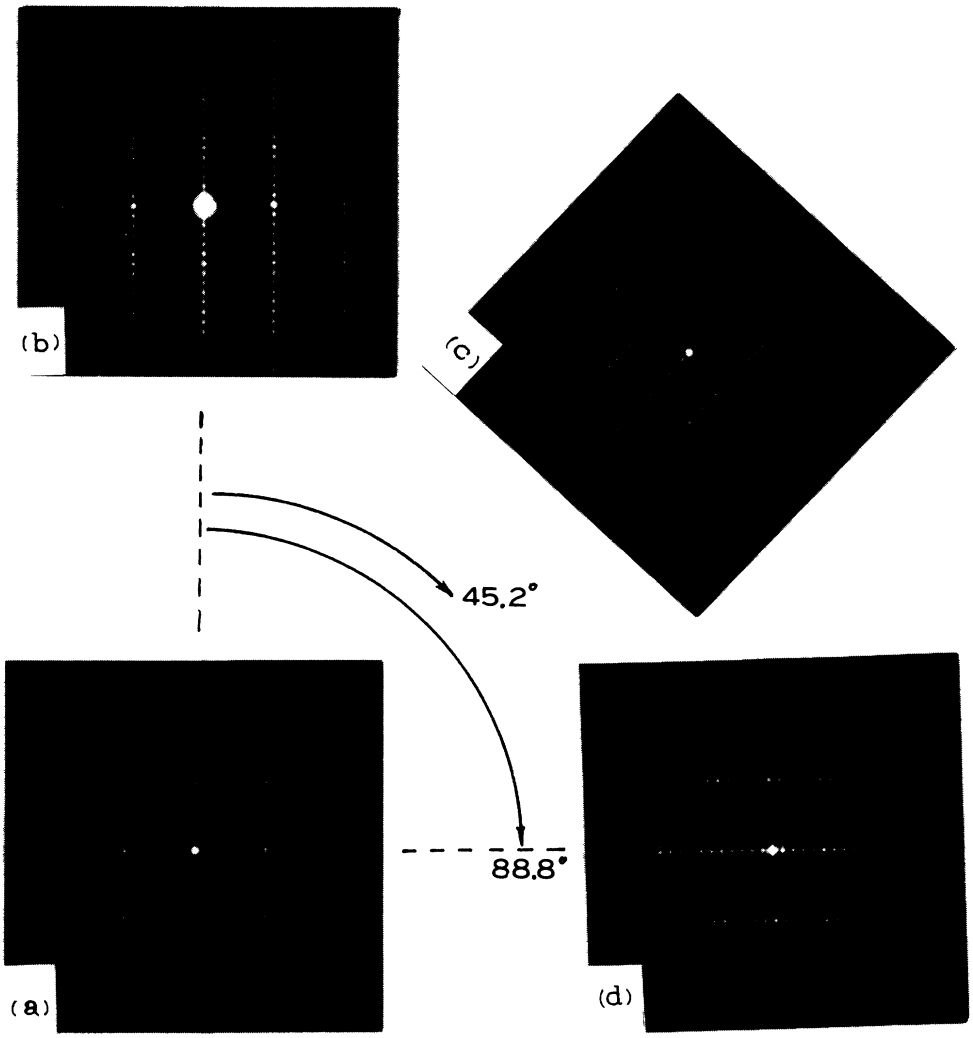

FIG. 7. SAD patterns, (a) [001], (b) [110], (c) [100], (d) [1$\bar{1}$0]. The modulated structure can be observed obviously.

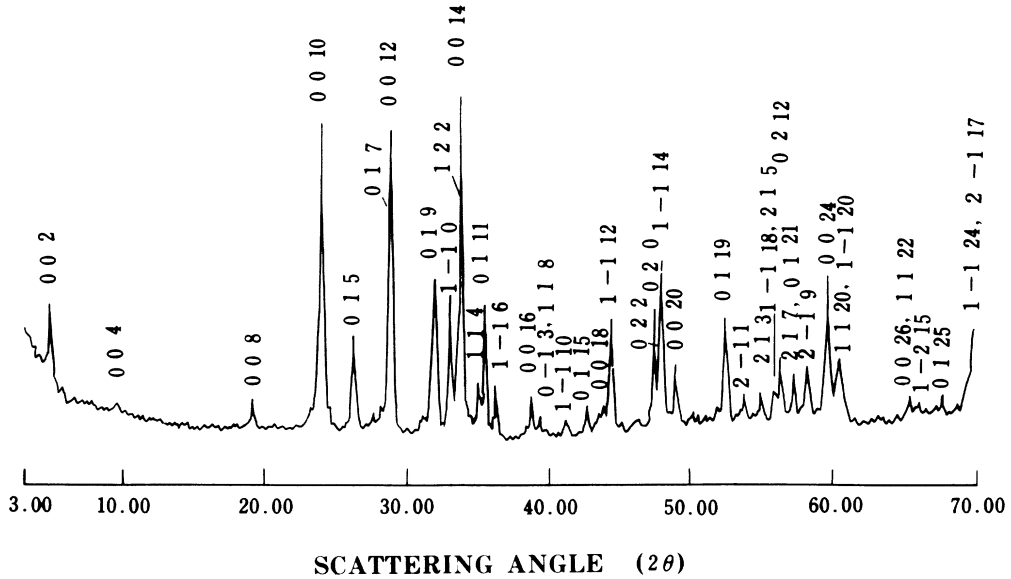

FIG. 8. XRD pattern of the 110-K monophase superconductor for CuK_α radiation. Reflections are assigned by monoclinic system.

The critical current density J_c, measured by a standard four-probe I-V method, of the single-phase sample reached up to 450 A/cm^2 (0 T, 77 K, 1 mm^2). It would be raised much higher if the density and/or grains orientation of the samples can be further improved.

In addition, the pressure dependence of superconductivity of the single-phase sample has also been studied. The critical temperatures increase with increasing pressure and the pressure derivative is 0.7 K/GPa. It is believed that the primary factors sensitive to pressure are the perfection of lattice and the distance among Cu-O layers. Besides, the jump of normal resistance near 1.0 GPa was observed and may be caused by some change in fine structure related to Cu-O layers.

ACKNOWLEDGMENTS

The authors would like to express deep gratitude to Q. Lin, Y. S. Du, L. Tang, Z. S. Ma, T. J. Zhu, S. L. Li, J. Li, and S. Y. Xia for their cooperation and support.

[1]J. G. Bednorz and K. A. Muller, Z. Phys. B **64**, 189 (1986).
[2]H. Maeda, Y. Tanaka, M. Fukutomi, and T. Asano, Jpn. J. Appl. Phys. **27**, L209 (1988).
[3]Z. Z. Sheng and A. M. Hermann, Nature **332**, 55 (1988); **332**, 138 (1988).
[4]C. Michel *et al.*, Z. Phys. B **68**, 421 (1987).
[5]J. M. Tarascon *et al.*, Phys. Rev. B **38**, 2504 (1988); **38**, 8885 (1988).
[6]S. A. Sunshine *et al.*, Phys. Rev. B **38**, 893 (1988).
[7]F. Shi *et al.*, Mod. Phys. Lett. B **3**, 571 (1989).
[8]S. Koyama, U. Endo, and T. Kawai, Jpn. J. Appl. Phys. **27**, L1861 (1988).
[9]T. S. Rong *et al.*, Appl. Phys. Lett. **54**, 2157 (1989).
[10]C. G. Cui *et al.*, Solid State Commun. **70**, 287 (1989).
[11]K. Kumagia and Y. Nakamura, Physica **157C**, 307 (1989).
[12]M. Sera, S. Kondoh, F. Fukuda, and M. Sato (unpublished).
[13]F. Seidler *et al.*, Physica **157C**, 375 (1989).
[14]R. Y. Jin, G. M. Zhao, and Q. Z. Ran, Solid State Commun. **67**, 415 (1988).
[15]M. Ishikawa, T. Takataka, and Y. Nakawaza, Physica **148B**, 332 (1987).
[16]C. Chen *et al.*, Solid State Commun. **68**, 749 (1988).

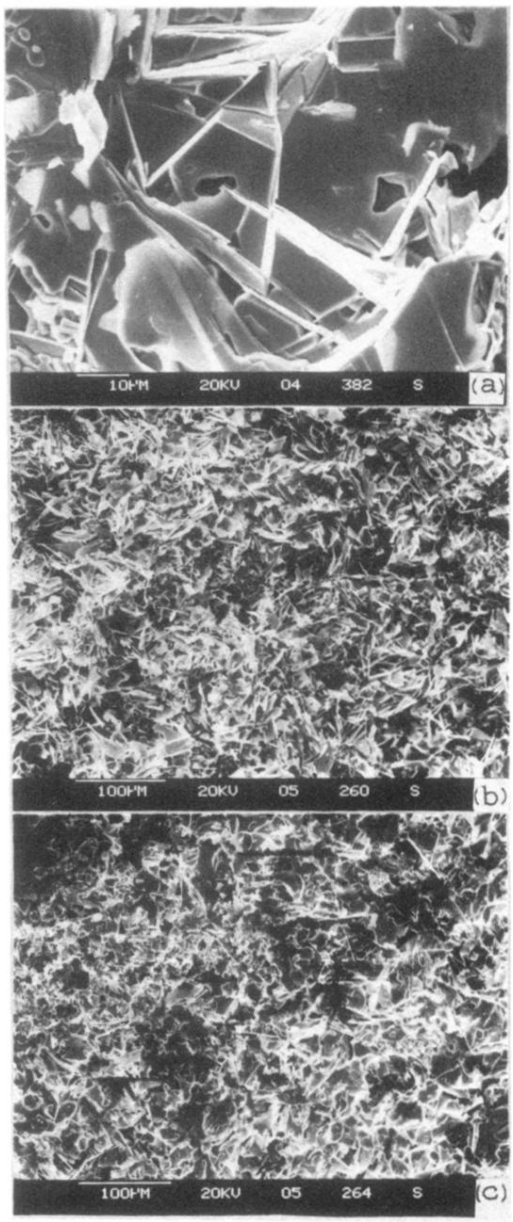

FIG. 2. SEM photos of the sample: (a) fractured surface with higher magnification; (b) fractured surface with lower magnification; (c) free surface with the same magnification as photo (b).

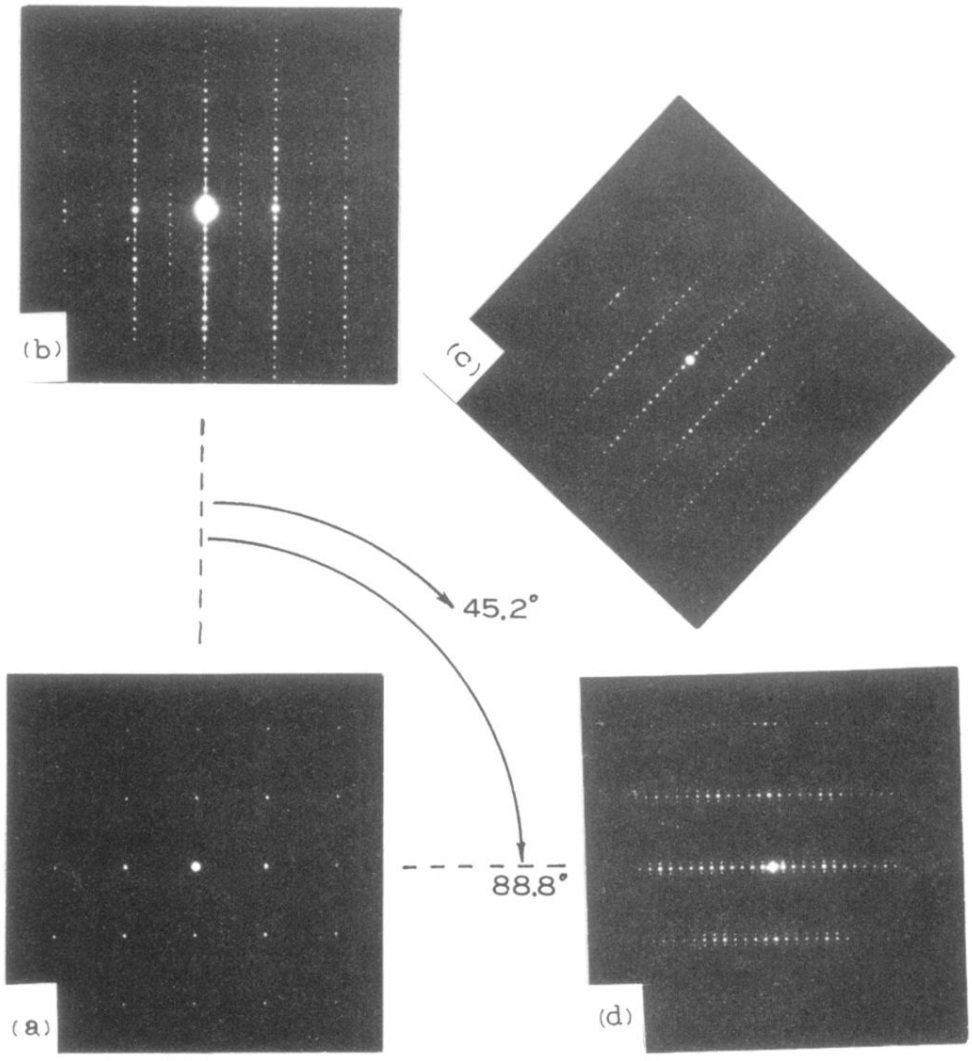

FIG. 7. SAD patterns, (a) [001], (b) [110], (c) [100], (d) [$1\bar{1}0$]. The modulated structure can be observed obviously.